Cloud droplet sedimentation, entrainment efficiency, and subtropical stratocumulus albedo

C. S. Bretherton,[1] P. N. Blossey,[1] and J. Uchida[2]

Received 27 July 2006; revised 25 October 2006; accepted 19 December 2006; published 9 February 2007.

[1] The effect of cloud droplet sedimentation on the entrainment rate and liquid water path of a nocturnal nondrizzling stratocumulus layer is examined using large-eddy simulations (LES) with bulk microphysics. In agreement with a prior study by Ackerman et al. (2004), sedimentation is found to decrease entrainment rate and thereby increase liquid water path. They suggested this is due to reduction of boundary-layer turbulence. Our simulations suggest otherwise. Instead, sedimentation reduces entrainment by removing liquid water from the entrainment zone. This inhibits two mechanisms that promote the sinking of entrained air into the cloud layer–entrainment-induced evaporative cooling and longwave radiative cooling. A sensitivity study shows that the radiative effect is less important than the reduced evaporation. A possible parameterization of the effect of sedimentation on entrainment rate in a mixed layer model is proposed and tested. Since the droplet sedimentation rate is inversely related to cloud droplet (and presumably aerosol) concentration and nearly nondrizzling marine stratocumulus are widespread, sedimentation impacts on stratocumulus entrainment efficiency should be considered in climate model simulations of the aerosol indirect effect. **Citation:** Bretherton, C. S., P. N. Blossey, and J. Uchida (2007), Cloud droplet sedimentation, entrainment efficiency, and subtropical stratocumulus albedo, *Geophys. Res. Lett.*, *34*, L03813, doi:10.1029/2006GL027648.

1. Introduction

[2] Recently, *Ackerman et al.* [2004] showed that sedimentation of cloud droplets in stratocumulus-capped mixed layers, a process neglected in most prior LES simulations, appreciably reduces the simulated entrainment rate into such layers. If the overlying air is much warmer and drier, as typical of the subtropical marine stratocumulus regions, the reduced entrainment causes the simulated cloud to appreciably thicken. Conversely, higher CCN concentrations can decrease the typical cloud droplet size and fall speed, decrease sedimentation and increase entrainment, resulting in a thinner cloud layer for more polluted conditions. Such cloud thinning can partly counteract the first indirect (Twomey) effect of enhanced aerosol concentration increasing the albedo of a cloud of fixed liquid water path, with important consequences for climate change simulation.

[3] *Ackerman et al.* [2004] explained the impact of sedimentation on entrainment as follows: 'Precipitation dries out cloudy air in updrafts, which reduces the moisture available for evaporative cooling of downdrafts. Precipitation thus reduces the kinetic energy available in the boundary layer to entrain warmer air from above the temperature inversion'. In this paper, we critically examine this explanation by analyzing LES of a nocturnal nondrizzling stratocumulus cloud layer with and without sedimentation of cloud droplets. We confirm Ackerman et al.'s finding that addition of droplet sedimentation can significantly decrease the entrainment rate and thicken the cloud. However, using both LES results and theoretical arguments, we show that turbulence levels in the cloud layer remain unchanged, counter to Ackerman et al.'s argument. Instead we show that droplet sedimentation reduces the 'entrainment efficiency', a nondimensional measure of the entrainment rate for a given turbulence level and inversion strength, by depleting the cloud-top entrainment zone of liquid water, as suggested in a one-dimensional Lagrangian parcel modeling framework by *Considine and Curry* [1998]. We consider two entrainment-efficiency reducing mechanisms, and propose a new entrainment closure that accounts for sedimentation in a manner consistent with our simulations.

2. Methods

[4] The effect of cloud droplet sedimentation on entrainment is most cleanly explored for stratocumuli assumed to have no drizzle-size droplets. Our simulations follow the specifications of a recent LES intercomparison [*Stevens et al.*, 2005] by the GEWEX Cloud System Study (GCSS) Boundary Layer Cloud Working Group (BLCWG). This was based on airborne observations of a nocturnal non-precipitating stratocumulus-capped mixed layer during the first research flight (RF01) of the DYCOMS-II field experiment off the coast of California in July 2001 [*Stevens et al.*, 2003]. The initial state was a well-mixed 840 m deep boundary layer with a 620 m cloud base, capped by a 7 K inversion, with a stratified dry layer above. Mean subsidence $\overline{w}(z) = -Dz$ with $D = 3.75 \times 10^{-6}\mathrm{s}^{-1}$ was imposed. Turbulence was forced by idealized net radiative cooling tied to the cloud liquid water profile and specified surface heat fluxes. All participating LES models assumed no sedimentation or precipitation of liquid water. A 96×96 doubly-periodic horizontal grid with 35 m horizontal resolution was specified. Our simulations were performed with version 6.4 of the System for Atmospheric Modeling [*Khairoutdinov and Randall*, 2003]. We used a uniform vertical resolution of 5 m up to the domain top of 1600 m, with a sponge layer between 1100 m and a rigid lid at the domain top.

[1]Department of Atmospheric Sciences, University of Washington, Seattle, Washington, USA.
[2]Department of Applied Mathematics, University of Washington, Seattle, Washington, USA.

0094-8276/07/2006GL027648$05.00

Table 1. 3–8 Hour Mean Entrainment Rate, Cloud Liquid Water Path, Sub-Inversion Standard Deviation of Vertical Velocity, Convective Velocity, Across-Inversion Buoyancy Jump, Inversion Height, and Entrainment Efficiency for the Four LES Simulations, Along With Standard Errors Derived From Their Hourly Variability for NoSed, and Relevant Statistics for the Two Mixed-Layer Model Simulations

	NoSed	LoSed	HiSed	TrRad	StdErr	MLNoSed	MLHiSed
w_e, mm s^{-1}	5.33	5.17	4.94	5.04	0.07	3.68	3.34
LWP, g m^{-2}	32.6	36.0	39.5	39.4	0.4	81.2	90.3
σ_w^{inv}, m s^{-1}	0.30	0.30	0.30	0.30	0.003		
w_*, m s^{-1}	0.97	1.00	1.02	1.02	0.01	1.11	1.11
Δb, m s^{-2}	0.31	0.31	0.30	0.30	0.001	0.26	0.26
z_i, m	885	881	877	877	0.2	844	838
A	1.58	1.39	1.22	1.25	0.05	0.59	0.53

[5] For the subsequent GCSS-BLCWG case study on precipitating stratocumulus, A. Ackerman (personal communication, 2006) proposed a simple formulation of sedimentation flux appropriate for bulk microphysical models. It assumes that cloud liquid water mixing ratio q_c (which can be loosely regarded as liquid water in droplets of radius less than 20 μm, and which is generally treated as a separate water category in bulk microphysical parameterizations) is partitioned over a lognormal distribution $p(r)$ of droplet radii r with a geometric standard deviation σ_g and a total droplet number concentration N_d. Using Stokes' law for the fall speed of a cloud droplet, $w_t(r) = cr^2$,$c = 1.19 \times 10^8 \mathrm{m}^{-1}\mathrm{s}^{-1}$ [*Rogers and Yau*, 1989, p. 125], and integrating across the droplet size distribution, Ackerman derived the following expression for the downward precipitation flux of water due to sedimentation:

$$P = \int_0^\infty w(t)m(r)p(r)dr = c(3/[4\pi\rho_l N_d])^{2/3}(\rho q_c)^{5/3}\exp\left(5\ln^2\sigma_g\right). \quad (1)$$

[6] Here $m(r)$ is the mass of a spherical droplet of radius r, and ρ and ρ_l are the density of air and liquid water, respectively. The geometric standard deviation $\sigma_g (= \exp(\sigma)$, where σ is the standard deviation of the underlying normal distribution) is 1 for a monodisperse spectrum in which all droplets have identical radius. A larger σ_g corresponds to a broader distribution of radii. Ackerman suggested taking $\sigma_g = 1.5$. M. C. Van Zanten (personal communication, 2005) pointed out that that $\sigma_g = 1.2$ (which implies a sedimentation flux approximately half as large) better matches fluxes calculated from DYCOMS-II aircraft-observed stratocumulus cloud droplet size distributions (excluding drizzle-size drops) for RF02. These two values bracket the range of σ_g found in analyses of earlier aircraft-derived data sets [e.g., *Martin et al.*, 1994; *Hudson and Yum*, 1997; *Miles et al.*, 2000; *Wood*, 2000]. We chose $N_d =$ 140 cm^{-3} to match RF01 observations [*van Zanten et al.*, 2005].

3. Results

[7] We compared four eight-hour simulations, all identically initialized and forced following the GCSS-RF01 case study specifications [*Stevens et al.*, 2005]. Simulation NoSed assumed no droplet sedimentation. The remaining simulations are spun up identically to NoSed for two hours, after which droplet sedimentation is turned on. Simulations LoSed and HiSed used a droplet sedimentation flux of the form (1) with $\sigma_g = 1.2$ and 1.5.

[8] After the simulations branch at 2 hours, their horizontal-mean cloud top and base heights systematically diverge, reflecting differences in their entrainment rates w_e. Table 1 presents the hour 3–8 means of w_e and several other statistics. Table 1 also includes simulations to be discussed later–TrRad is a variation on HiSed, and MLNoSed and MLHiSed are mixed-layer model simulations. For all tabulated statistics, uncertainty estimates were calculated for NoSed by regarding the hour 3–8 mean as an estimate based on ten averages over 30 minute periods ($\sim 2z_i/w_*$, or two eddy turnover times) and detrending this time series to obtain residual variability from which the standard error σ of their estimated mean is derived (Table 1, column StdErr). These uncertainty estimates are also representative of the other simulations.

[9] Our LES simulations corroborate Ackerman's finding that stronger droplet sedimentation leads to less entrainment and a thicker cloud layer. The HiSed w_e is 7% less than for NoSed, with LoSed (which has half the sedimentation flux as HiSed for the same q_c and N_d) having half as large an entrainment rate reduction when compared to NoSed. The entrainment rate w_e is derived from the inversion height $z_i(t)$, calculated as the mean height of the 8 g kg^{-1} total water isosurface as in the GCSS case specification. The 4σ decrease in w_e between NoSed and HiSed is highly statistically significant. Table 1 also shows less entrainment leads to higher liquid water path (LWP) in simulations with stronger sedimentation.

[10] The next tabulated statistic, σ_w^{inv}, is the root mean square value of the vertical velocity perturbation w' in the 50 m below the inversion, and measures the strength of eddies impinging on the inversion. This is nearly identical in all the simulations, at odds with *Ackerman et al.*'s [2004] assertion that the reduction of entrainment by sedimentation is due to a reduction in the turbulent kinetic energy available for entrainment.

[11] Table 1 also shows several other parameters commonly used in scaling and parameterizing entrainment. Convective velocity w_* measures the buoyancy forcing of turbulence integrated over the boundary layer depth:

$$w_* = \left(2.5\int_0^\infty \overline{w'b'}dz\right)^{1/3}.$$

[12] Here, an overline denotes a horizontal average and b' is the buoyancy perturbation (including liquid water loading) from the horizontal mean. Table 1 shows that w_* is about 5% larger in HiSed than in NoSed. It also indicates that both Δb, the virtual temperature jump across the inversion scaled into a buoyancy, and the inversion height z_i vary little between runs because they have insufficient time to drift significantly.

[13] Lastly, $A = w_e\ \Delta b\ z_i/w_*^3$ is a nondimensional entrainment efficiency. For a surface-heated dry convective boundary layer, $A \approx 0.2$, but observational estimates of A for a stratocumulus-topped boundary layer are typically

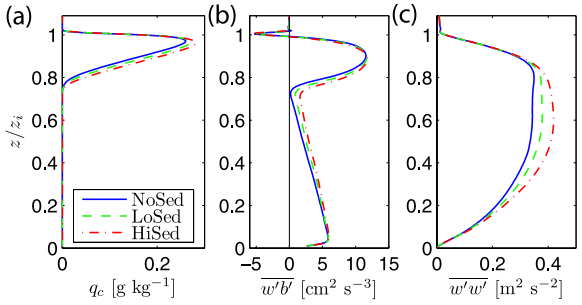

Figure 1. 3–8 hour mean profiles of (a) liquid water mixing ratio, (b) buoyancy flux and (c) vertical velocity variance vs. normalized height z/z_i (as defined in text).

4–20 times larger [e.g., *Nicholls and Turton*, 1986]. This has been interpreted as enhancement of entrainment due to evaporative cooling of mixtures of cloudy and above cloud air and to cloud-top radiative cooling. We interpret the reduced entrainment efficiency in HiSed compared to NoSed as evidence that droplet sedimentation is affecting these processes.

[14] Figure 1 shows 3–8 hour mean profiles of liquid water content q_c, buoyancy flux $\overline{w'b'}$ and vertical velocity variance $\overline{w'^2}$. Before time-averaging, the vertical coordinate in each profile at each time is rescaled into a normalized inversion height $z/z_i(t)$.

[15] Sedimentation increases the cloud liquid water path but depletes water from the thin entrainment zone at the very top of the cloud, noticeably moving down and rounding off the q_c maximum. Below cloud base ($z/z_i < 0.8$), the buoyancy flux is slightly enhanced by sedimentation because of the reduced entrainment of warm air. Above cloud base, the buoyancy flux is slightly reduced. The resulting vertical velocity variance is essentially identical near cloud top in all simulations, but increases slightly with droplet sedimentation below cloud base. The maximum cloud fraction is near to one is all simulations.

4. Sedimentation and Turbulence

[16] Drizzle (precipitation of drops of larger radii that fall a significant distance below cloud base) stabilizes the boundary layer and reduces cloud-layer turbulence because latent heat is released by condensation in the cloud layer and given up to evaporation below the cloud [e.g., *Stevens et al.*, 1998]. Like drizzle, sedimentation moves liquid water downward, but unlike drizzle, none of this water gets below cloud base. This limits the direct impact of sedimentation on the boundary-layer diabatic heating profile.

[17] This can be quantified by considering a mixed-layer idealization in which moist static energy h and total water q_t are uniform within the boundary layer, their mean horizontal advection is neglected, and we make the Boussinesq approximation with a constant reference density ρ_r. Following the discussion and notation of *Bretherton and Wyant* [1997], this implies that within the boundary layer, the total energy flux $E(z) = \overline{w'h'} + F_{rad}/\rho_r$ and the total water flux $W(z) = \overline{w'h'} - P(z)$ are linear functions of z. Defining $\zeta = z/z_i$, the vertical buoyancy flux profile can then be expressed as the sum of contributions from surface fluxes, entrainment, radiation, and precipitation:

$$\begin{aligned}\overline{w'b'}(z) &= c_h\overline{w'h'}(z) + c_q\overline{w'q_t'}(z)\\ &= c_h\left[E(z) - \rho_r^{-1}F_{rad}(z)\right] + c_q[W(z) + P(z)]\\ &= [1-\zeta]\left[c_hE(0) + c_qW(0)\right] + \zeta w_e[c_h\Delta h + c_q\Delta q]\\ &\quad - c_h\left[E(z) - \rho_r^{-1}F_{rad}(z)\right] + B_P(z). \end{aligned} \tag{2}$$

[18] The thermodynamic coefficients c_h and c_q, defined by *Bretherton and Wyant* [1997], have different values above and below cloud base z_b. The terms $E(0)$ and $W(0)$ include the surface fluxes, while Δ denotes an inversion jump.

[19] For our purposes, only the precipitation contribution

$$B_P(z) = c_q[P(z) - (1 - z/z_i)P(0)] \tag{3}$$

is important. If sedimentation is the only form of precipitation, $P(z)$ is zero below cloud base. Above cloud base, $c_q = -g$, where g is the gravitational acceleration, so

$$B_P(z) = \begin{cases} -gP(z), & z > z_b, \\ 0, & z < z_b. \end{cases} \tag{4}$$

[20] Physically, buoyancy production is slightly diminished because turbulence must resupply gravitational potential energy lost in sedimenting droplets. However, a comparable drizzle flux falling below cloud base induces a much larger buoyancy flux reduction, because $c_q/g = -0.93L/(c_pT)$ is approximately 8 times larger in magnitude than within the cloud due to evaporative cooling. This is illustrated in Figure 2, which compares the precipitation flux and precipitation-induced buoyancy production profiles for idealized sedimenting and drizzling stratocumulus-capped mixed layers.

[21] Thus for a given w_e, drizzle can significantly reduce boundary layer turbulence while sedimentation has a much smaller effect. However, we have seen that sedimentation *can* nevertheless substantially reduce entrainment, creating an indirect but profound impact on the depths of the boundary layer and the cloud.

5. Sedimentation and Entrainment

[22] Sedimentation depletes liquid water from the entrainment zone at the stratocumulus cloud top. Two mechanisms

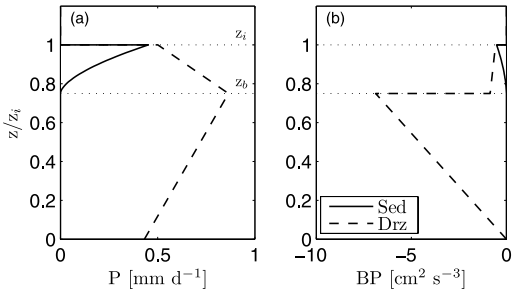

Figure 2. Profiles of (a) precipitation flux $P(z)$ and (b) precipitation contribution $B_P(z)$ to buoyancy flux for idealized sedimenting non-drizzling (Sed) and drizzling (Drz) cloud-topped mixed layers.

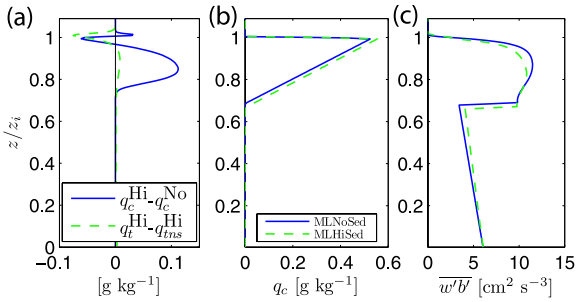

Figure 3. 3–8 hour LES mean profiles of (a) HiSed - NoSed difference of normalized q_c and the difference for HiSed of q_t and q_{tns} (the nonsedimenting water tracer) and 5.5 hour mixed-layer model profiles of (b) liquid water mixing ratio and (c) buoyancy flux vs. normalized height z/z_i.

by which this may reduce entrainment are (1) reduced potential for evaporative enhancement of entrainment and (2) reducing cloud-top radiative cooling within the entrainment zone. LES results presented in this section suggest that the first mechanism is more important than the second.

[23] Figure 3a quantifies the depletion of liquid water by sedimentation out of the entrainment zone. The solid curve shows the profile of the difference in q_c between HiSed and NoSed. In the entrainment zone ($z/z_i > 0.98$), the mean q_c is up to 0.07 g kg^{-1} less in HiSed than in NoSed. We interpret this depletion as due to sedimentation. This interpretation is supported by adding to HiSed a nonsedimenting total water tracer q_{tns}, which is initialized and forced identically to q_t except for neglect of the sedimentation flux. The dashed curve in Figure 3a shows that in the entrainment zone, the minimum of $q_t - q_{tns}$ is -0.08 g kg^{-1}, comparable to the above liquid water depletion. This agreement holds despite other obvious differences in the two profiles. Greater variability of the inversion height in HiSed leads to the secondary peak in the q_c difference above $z = z_i$, and in the mixed layer ($z/z_i < 0.98$), less entrainment in HiSed increases q_c compared to LoSed.

[24] To assess the importance of radiative cooling feedbacks, we performed simulation TrRad, which is identical to HiSed except that the radiative cooling profile is computed using liquid water q_{cns} based on the nonsedimenting water tracer q_{tns} in place of the actual q_t. This removes the radiative feedback of sedimentation while retaining its evaporative feedback. Table 1 shows that the differences in entrainment efficiency between TrRad and HiSed are roughly 10% as large as those between NoSed and HiSed. This suggests that evaporative feedbacks account for about 90% of the entrainment reduction by sedimentation.

6. Sedimentation in Entrainment Closure

[25] Our set of simulations is too limited to form a reliable basis for a definitive parameterization of sedimentation feedbacks in a large-scale weather or climate prediction model which does not resolve stratocumulus inversion layers. Nevertheless, combining our simulation results with physical reasoning, we produce a plausible modification to accounts for sedimentation in one entrainment closure, as follows. We assume that the entrainment-zone liquid water content is depleted by a fraction that depends on the ratio of the sedimentation flux out of the entrainment zone to the liquid water flux supplied by turbulent updrafts into this layer. A scaling argument suggests that this ratio should scale as w_{sed}/w_{turb}, where $w_{sed} = P(\overline{z_i})/(\rho q_c)$ is the droplet terminal velocity weighted over the droplet size-spectrum, and w_{turb} is an in-cloud turbulent updraft velocity. The one-dimensional model of *Considine and Curry* [1998] also suggested this dependence, but did not consider the feedback of entrainment zone liquid water depletion on the entrainment rate that is the central focus of this paper.

[26] As an example of how to account for this feedback, we consider the Nicholls-Turton closure [*Nicholls and Turton*, 1986]:

$$w_e = A w_*^3/(\Delta b\, z_i),\ A = 0.2(1 + a_2\, \chi_s\, J). \tag{5}$$

[27] The turbulent velocity w_{turb} of entraining eddies is assumed to scale with w_*. The entrainment efficiency A is increased at a cloud-top by the product of three factors–the mass fraction χ_s of above-inversion air necessary to evaporate a mixture of above-cloud and mixed layer air (proportional to mixed-layer-top liquid water content), a nondimensional measure $J = 1 - (db/d\chi)_s/\Delta_b$ of the reduction in buoyancy by evaporation when a parcel of cloudy mixed layer air is diluted by a small amount of above-inversion air, and an evaporative enhancement coefficient a_2. *Nicholls and Turton* [1986] suggested $a_2 = 60$, but recent observations [*Caldwell et al.*, 2005; *Stevens et al.*, 2005] support our choice $a_2 = 15$.

[28] To account for the reduction in entrainment-zone liquid by sedimentation, we replace χ_s in (5) by

$$\chi_{sed} = \chi_s \exp\left(-a_{sed} w_{sed}/w_*\right) \tag{6}$$

where a_{sed} is an empirically-chosen nondimensional constant. The choice of an exponential functional form is arbitrary, but has the proper limiting behavior that extremely large sedimentation removes all liquid water from the inversion and reduces the entrainment efficiency to its dry value, while extremely weak sedimentation has no effect on entrainment. Since w_e depends directly on the droplet concentration through w_{sed}, this entrainment closure can reproduce *Ackerman et al.*'s [2004] key result that enhanced aerosol can cause thinning of a nondrizzling stratocumulus layer capped by a dry free troposphere.

[29] SAM, like most other LESs, has excessive entrainment efficiency compared to observations for the GCSS RF01 case [*Stevens et al.*, 2005] and other stratocumulus-topped mixed layers, and this may also bias its simulation of sedimentation impacts on entrainment rate. Nevertheless, lacking better data, we use the LES output to tune the parameter a_{sed} in (6) as follows.

[30] We run a mixed layer model [*Bretherton and Wyant*, 1997] initialized and forced identically to the LES, except for replacing the above-inversion thermal structure with a fixed inversion-top potential temperature of 299.5 K to roughly match the LES-simulated inversion temperature jump. Run MLNoSed uses the nonsedimenting entrainment closure (5). We then add the sedimentation modification (6) to the entrainment closure, giving a new 3–8 hour mean

entrainment rate w_e(MLHiSed) which depends on a_{sed}. We insist that w_e(MLHiSed)/w_e(MLNoSed) = 0.93, the value derived from the LES simulations of Table 1. This obtains when a_{sed} = 9. Figures 3b and 3c show profiles of liquid water and buoyancy flux for the mixed-layer model simulations MLNoSed and MLHiSed at 5.5 hours for comparison with the 3–8 hour LES mean profiles in Figures 1a and 1b. In the mixed-layer model, as in the LES, q_l and $\overline{w'b'}$ are larger in the sedimenting run, reflecting the feedbacks of reduced entrainment. Table 1 shows bulk statistics from the two mixed-layer runs, which have similar sensitivity to sedimentation as the LES, though with lower and more realistic entrainment rate and higher LWP.

[31] These simulations and those of *Ackerman et al.* [2004] suggest that moist turbulence parameterizations used in climate model simulations of the first aerosol indirect effect should account for sedimentation effects on entrainment efficiency, as they may have significant effects on liquid water path for typical marine cloud droplet concentrations. However, some issues pertinent to the functional form and choice of turbulent velocity scale used in our proposed entrainment closure need further investigation. First, the simulations presented here are too limited to rigorously test (6). They have nearly identical w_*, so they are inadequate to check that the dependence of entrainment on sedimentation operates only through the nondimensional ratio w_{sed}/w_*. The fractional reduction of entrainment rate is too small to check that an exponential dependence in (6) is appropriate. These latter two assumptions are physically plausible but should be tested using LES across a wider range of parameter space. In addition, it will be important to test whether a_{sed} is sensitive to the choice of LES. Lastly, while w_* increases between NoSed and HiSed, σ_w^{inv} does not, because the buoyancy flux increase is all below cloud base. A more skillful predictor of σ_w^{inv}, such as the *Lilly* [2002] closure, which weights buoyancy production with z/z_i to estimate a top-weighted turbulent velocity scale, might be a preferable turbulent velocity scale for the entrainment closure.

[32] **Acknowledgments.** We thank R. Wood A. Ackerman, and B. Stevens for useful conversations about this work, and M. Khairoutdinov for providing SAM. This work was supported by NASA grant NAG5-13564 and NSF grant ATM-0433712.

References

Ackerman, A., M. P. Kirkpatrick, D. E. Stevens, and O. B. Toon (2004), The impact of humidity above stratiform clouds on indirect aerosol climate forcing, *Nature*, *432*, 1014–1017.

Bretherton, C. S., and M. C. Wyant (1997), Moisture transport, lower-tropospheric stability, and decoupling of cloud-topped boundary layers, *J. Atmos. Sci.*, *54*, 148–167.

Caldwell, P., C. S. Bretherton, and R. Wood (2005), Mixed-layer budget analysis of the diurnal cycle of entrainment in SE Pacific stratocumulus, *J. Atmos. Sci.*, *62*, 3775–3791.

Considine, G., and J. A. Curry (1998), Effects of entrainment and droplet sedimentation on the microphysical nature of stratus and stratocumulus clouds, *Q. J. R. Meteorol. Soc.*, *124*, 123–150.

Hudson, J. G., and S. S. Yum (1997), Droplet spectral broadening in marine stratus, *J. Atmos. Sci.*, *54*, 2642–2654.

Khairoutdinov, M. F., and D. A. Randall (2003), Cloud resolving modeling of the ARM summer 1997 IOP: Model formulation, results, uncertainties, and sensitivities, *J. Atmos. Sci.*, *60*, 607–625.

Lilly, D. K. (2002), Entrainment into cloud-topped mixed layers: II. A new closure, *J. Atmos. Sci.*, *59*, 3353–3361.

Martin, G. M., D. W. Johnson, and A. Spice (1994), The measurement and parameterization of effective radius of droplets in warm stratocumulus clouds, *J. Atmos. Sci.*, *51*, 1823–1842.

Miles, N. L., J. Verlinde, and E. E. Clothiaux (2000), Cloud droplet size distributions in low-level stratiform clouds, *J. Atmos. Sci.*, *57*, 295–311.

Nicholls, S., and J. D. Turton (1986), An observational study of the structure of stratiform cloud sheets: part II. Entrainment, *Q. J. R. Meteorol. Soc.*, *112*, 461–480.

Rogers, R. R., and M. K. Yau (1989), *A Short Course in Cloud Physics,* 3rd ed., 290 pp., Elsevier, New York.

Stevens, B., W. R. Cotton, G. Feingold, and C.-H. Moeng (1998), Large-eddy simulations of strongly precipitating, shallow, stratocumulus-topped boundary layers, *J. Atmos. Sci.*, *55*, 3616–3638.

Stevens, B., et al. (2003), On entrainment rates in nocturnal marine stratocumulus, *Q. J. R. Meteorol. Soc.*, *129*, 3469–3493.

Stevens, B., et al. (2005), Evaluation of large-eddy simulations via observations of nocturnal marine stratocumulus, *Mon. Weather Rev.*, *133*, 1443–1462.

van Zanten, M. C., B. Stevens, G. Vali, and D. H. Lenschow (2005), Observations of drizzle in nocturnal marine stratocumulus, *J. Atmos. Sci.*, *62*, 88–106.

Wood, R. (2000), Parameterization of the effect of drizzle upon the droplet effective radius in stratocumulus clouds, *Q. J. R. Meteorol. Soc.*, *126*, 3309–3324.

P. N. Blossey and C. S. Bretherton, Department of Atmospheric Sciences, University of Washington, Box 351640, Seattle, WA 98195-1640, USA. (breth@atmos.washington.edu)

J. Uchida, Department of Applied Mathematics, University of Washington, Seattle, WA 98195, USA.